

Identification of GDF15 peptide fragments inhibiting GFRAL receptor signaling

Flora Alexopoulou^{a,b}, Nina Buch-Månson^a, Søren Ljungberg Pedersen^{a,1}, Niels Vrang^a,
Lisbeth Nielsen Fink^a, Kristian Strømgaard^{b,*}

^a Gubra Aps, Hørsholm, DK-2970 Hørsholm, Denmark

^b Department of Drug Design and Pharmacology, University of Copenhagen, DK-2100 Copenhagen, Denmark

ARTICLE INFO

Keywords:

Peptide technologies
GDF15
GFRAL
Peptide inhibitors
Cachexia

ABSTRACT

Growth differentiation factor 15 (GDF15) is believed to be a major causative factor for cancer-induced cachexia. Recent elucidation of the central circuits involved in GDF15 function and its signaling through the glial cell-derived neurotrophic factor family receptor α -like (GFRAL) has prompted the interest of targeting the GDF15-GFRAL signaling for energy homeostasis and body weight regulation. Here, we applied advanced peptide technologies to identify GDF15 peptide fragments inhibiting GFRAL signaling. SPOT peptide arrays revealed binding of GDF15 C-terminal peptide fragments to the extracellular domain of GFRAL. Parallel solid-phase peptide synthesis allowed for generation of complementary GDF15 peptide libraries and their subsequent functional evaluation in cells expressing the GFRAL/RET receptor complex. We identified a series of C-terminal fragments of GDF15 inhibiting GFRAL activity in the micromolar range. These novel GFRAL peptide inhibitors could serve as valuable tools for further development of peptide therapeutics towards the treatment of cachexia and other wasting disorders.

1. Introduction

Growth differentiation factor 15 (GDF15) was first described in 1997 [1–3] as a 25 kDa dimeric secreted hormone bearing common three-dimensional structural characteristics with the transforming growth factor β (TGF- β) superfamily. GDF15 is expressed in various tissues such as liver, lung, kidney, and placenta [4], and elevated serum levels of GDF15 are associated with a variety of physiological conditions including age, pregnancy, and exercise [5–7]. Additionally, serum GDF15 positively correlates with inflammation [8] in chronic diseases such as cancer [9], cardiovascular disease [10], chronic kidney [11] and liver diseases [12], as well as in viral infections [13]. Accumulating experimental evidence has linked GDF15 with energy intake regulation and weight maintenance while increased circulating GDF15 levels in obesity have been suggested as a compensatory molecular mechanism to reduce energy intake [14].

Notably, GDF15 has been proposed as a causative factor for development of cancer cachexia [15]. Cachexia describes a metabolic wasting syndrome characterized by unintended weight loss accompanied by

impaired regulation of energy homeostasis and progressive depletion of skeletal muscle [16,17]. Impaired energy homeostasis is triggered by both the tumor and its treatment (e.g. radiation, chemotherapy) and involves combinations of metabolic abnormalities in various signaling pathways [18,19]. The multifactorial metabolic aetiology of cachexia hampers the efficacy of current treatments based on nutritional supplements and appetite stimulants, leaving a large and unmet medical need for more efficacious and targeted therapies [20,21].

Until recently, the molecular mechanism through which GDF15 promotes body weight loss has remained elusive. In 2017, four research groups independently identified the GDNF family receptor α -like (GFRAL) as the principal receptor mediating the metabolic effects of GDF15 [22–25]. Consistent with the inhibitory effects of GDF15 on appetite function, GFRAL expression was found to be highly restricted to the brainstem, specifically in neurons of the area postrema (AP) and the nucleus of the solitary tract (NTS), brain regions highly associated with central control of energy homeostasis [23,25]. GDF15 binds specifically and with high affinity to GFRAL, while recruitment of co-receptor RET, a receptor tyrosine kinase, and formation of the GDF15/GFRAL/RET

* Correspondence to: Department of Drug Design and Pharmacology, University of Copenhagen, Universitetsparken 2, DK-2100 Copenhagen, Denmark.
E-mail address: kristian.stromgaard@sund.ku.dk (K. Strømgaard).

¹ Present address: Pephexia Therapeutics ApS, Ole Maaløes Vej 3, DK-2200 Copenhagen, Denmark.

ternary complex is required for intracellular signaling. Conversely, metalloproteinase-mediated inactivation of GFRAL has recently been reported to negatively regulate GDF15-GFRAL signaling [26]. Interestingly, GFRAL knock-out mice are resistant to chemotherapy-induced weight loss, supporting a role of GFRAL signaling in cancer cachexia [22]. Moreover, GDF15-induced appetite suppression in rats was prevented by co-administration of an anti-GFRAL antibody [25]. Collectively, these findings strengthen the concept of inhibiting GDF15-GFRAL activity for the treatment of cachexia.

To date, the focus of targeting GFRAL function has been largely related to the treatment of obesity. Accordingly, several pharmaceutical companies have developed clinically relevant GDF15-based peptide therapeutics for obesity management including recombinantly expressed long-acting GDF15 analogues [27,28]. Despite that currently no FDA-approved medications for the indication of cancer cachexia are available, to our knowledge, limited efforts have been made to identify modalities for inhibiting GDF15 function in cachexia. The clinical relevance of targeting the GDF15-GFRAL axis for cachexia is supported by several preclinical studies. For example, administration of monoclonal antibodies neutralizing GDF15-induced signaling have been demonstrated to reverse the cachectic phenotype in transgenic mice overexpressing GDF15 [15] and prevent weight loss in tumor-bearing mice [29–31]. Here, we report the identification of GDF15 peptide fragments inhibiting GFRAL signaling and providing templates for the development of novel peptide-based therapeutics of cachexia targeting GDF15/GFRAL/RET signaling.

2. Materials and methods

2.1. SPOT arrays

SPOT peptide arrays (CelluSpots, Intavis AG, Cologne, Germany) were synthesized using a RePepSL synthesizer (Intavis AG, Tübingen, Germany) on cellulose membrane discs (Intavis AG) containing a 9-fluorenylmethoxycarbonyl- β -alanine (Fmoc- β -Ala) linker. Synthesis was initiated by Fmoc deprotection using 20 % piperidine in *N*-methylpyrrolidone (NMP) followed by washing with dimethylformamide (DMF) and ethanol (EtOH). Peptide synthesis was performed using coupling solution consisting of preactivated amino acids (0.5 M) with ethyl (hydroxyimino)cyanoacetate (Oxyma) (1.5 M) and *N,N*-diisopropylcarbodiimide (DIC, 1.1 M) in NMP. After 4 coupling rounds the membrane was capped twice with capping mixture (5 % acidic anhydride in NMP). Final Fmoc deprotection was followed by *N*-terminal acetylation with capping mixture, DMF and EtOH wash.

Dried cellulose membrane discs of cleavable synthesized peptides were transferred into Eppendorf tubes and treated with side chain deprotection solution (80 % TFA, 12 % DCM, 5 % H₂O, and 3 % triisopropylsilane (TIPS)) for 1.5 h at room temperature (RT). Discs were then removed, cleaved peptides were precipitated with cold diethyl ether and pelleted at 14000g (4 °C, 15 min). Peptides were dissolved in 50:50:0.1 (CH₃CN:H₂O:TFA) and analysed using LC-MS.

Dried cellulose membrane discs were transferred to Eppendorf tubes and treated with side chain deprotection solution (80 % TFA, 12 % DCM, 5 % H₂O, and 3 % TIPS) for 1.5 h at RT. Deprotection solution was then removed and a solvation mixture (88.5 % TFA, 4 % trifluoromethanesulfonic acid (TFMSA), 5 % H₂O, and 2.5 % TIPS) was added for overnight solubilization of the discs. Peptide-cellulose conjugates were then precipitated with cold diethyl ether and pelleted at 3000 rpm for 15 min, followed by an additional wash with cold ether. DMSO stocks of the conjugates were prepared and transferred to a 384-well plate for printing (in duplicates) on white coated CelluSpots blank slides (76 × 26 mm, Intavis AG) using a SlideSpotter robot (Intavis AG, Tübingen, Germany).

Printed slides were washed (2 ×) with PBS and incubated with 1 % bovine serum albumin (BSA) in PBS for 4 h. Slides were then washed with 1 % BSA in PBS (5 ×) and incubated with 0.1 μ M GFRAL His-tagged

extracellular domain (ECD) (Catalog# 9647-GR-050, R&D systems) in 1 % BSA in PBS for 1 h. Washing (4x) with 1 % BSA in PBS was followed by incubation with HRP anti-6x His-tag Ab (1:5000 dilution, Catalog# ab184607, Abcam) for 30 min. Lastly, slides were washed (4x) with 1 % BSA in PBS, (2 ×) with PBS and the detection substrate was (SuperSignal™ West Femto Maximum Sensitivity Substrate, Catalog# 34095, Thermo Scientific) added to the slides. Slides were visualized with a Syngene PXi image recorder (exposure time = 5 s). The resulting blots were analyzed using the Array Analyze Software (Active Motif), which defines the error range of each data set by comparing the intensities of each peptide duplicate on the analyzed array.

2.2. Peptide synthesis

Reagents for solid-phase peptide synthesis (SPPS) were purchased from Iris Biotech GmbH (Marktredwitz, Germany). Milli-Q water (Merck Millipore) was used for all experiments. Peptides were synthesized using fully automated Syro-II peptide synthesizer (MultiSynTech GmbH, Witten, Germany) by SPPS according to the 9-fluorenylmethoxycarbonyl (Fmoc) strategy. Peptide synthesis was conducted on 0.008–0.2 mmol scale using TentaGel S RAM resin (0.24 mmol/g) as solid support. Fmoc-protected amino acids (4 eq.) were coupled using DIC (4 eq.) and ethyl Oxyma (4 eq.) in DMF, except Fmoc-Phe-OH, which was dissolved in NMP. All couplings were performed at 75 °C for 10 min, except His and Cys which were performed at 50 °C for 15 min, either as single or as double couplings. Fmoc deprotection was performed using 20 % piperidine in DMF and 0.1 M HOBt was added to avoid aspartimide formation. Release of peptide from the solid support and simultaneous removal of the acid-labile side chain protecting groups was performed by incubation with a trifluoroacetic acid (TFA):triethylsilane:H₂O (95:2.5:2.5) mixture for 3 h at RT. The peptides were precipitated using cold diethyl ether.

Crude peptides were purified by preparative RP-HPLC (Prep. 150-LC, Waters, Taastrup, Denmark) using a C18 column (5 μ m, 110 Å, 21.2 × 30 mm, Dr. Maisch GmbH) and a solvent system containing solvent A (H₂O + 0.1 % TFA) and solvent B (CH₃CN + 0.1 % TFA). B gradient elution was applied at a flow rate of 20 ml/min and column effluent was monitored by UV absorbance at 215 nm and 254 nm. Peptide purity was determined by LC-MS (SQ detector 2 and Acquity UPLC, Waters, Taastrup, Denmark) and aliquotation was performed after concentration determination using Vanquish™ Charged Aerosol Detector (CAD, Thermo Fisher Scientific, Waltham, MA USA).

2.3. Cell culture

HEK293 cells (Catalog# 85120602, ECACC) were cultured at 37 °C, 5 % CO₂, and > 95 % humidity in DMEM/F-12 supplemented with GlutaMAX (Catalog# 41090093, Thermo Scientific), 1 % MEM Non-Essential Amino Acids Solution (Catalog# 1140035, Thermo Scientific), 10 % FBS (Catalog# 16140071, Thermo Scientific), 1 % Penicillin/Streptomycin (Catalog# P4333, Sigma-Aldrich). HEK293 cells were transfected with *h*GFRAL (Catalog# SC1200, Genscript) using Turbofect (Catalog# 15325016, Thermo Scientific) according to manufacturer's instructions. 24 h after transfection, selection was started using 500 μ g/ml geneticin (Catalog# 10131-027, Thermo Scientific). Subcloning was performed on the surviving cells to obtain a monoclonal *h*GFRAL cell line. For maintenance of the stable monoclonal *h*GFRAL cells based on HEK293, 500 μ g/ml geneticin was added to the culture medium.

2.4. In vitro functional assay

HEK293 cells stably overexpressing the *h*GFRAL were seeded in a PDL-coated 96-well plate (Catalog# 354461, Corning) as 40,000 cells/well. After 24 h, cells were transfected with *h*RET (Catalog# HG11997-CM, Sino Biological) using Lipofectamine 2000 (Catalog# 11668019, Thermo Scientific) according to the manufacturer's instructions.

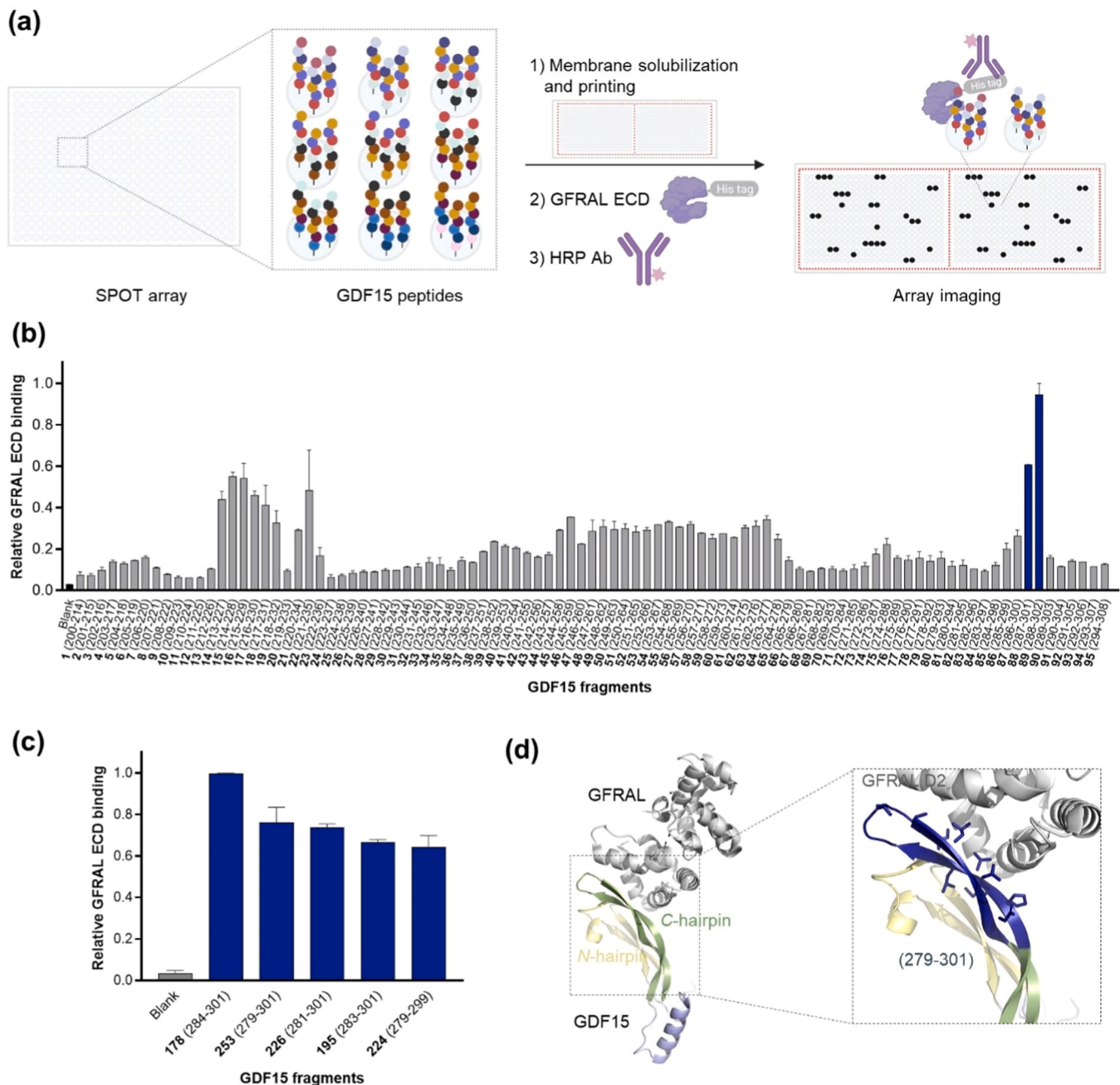


Fig. 1. GDF15 peptide fragments displayed on SPOT arrays bind to GFRAL ECD. **(a)** Schematic representation of a SPOT array. Immobilized GDF15 peptide fragments are screened against the His-tagged extracellular domain (ECD) of GFRAL. Incubation with a horseradish peroxidase (HRP) conjugated 6xHis antibody is followed by detection using a chromogenic substance. Black spots represent GDF15 fragments bound to GFRAL ECD. **(b)** Screening of SPOT array 1 displaying GDF15 15-mer fragments. **(c)** Top hits from screening of SPOT array 2 including 16–23-mer peptide fragments of the C-terminal hairpin of GDF15. **(d)** X-ray structure of GDF15 monomer in complex with GFRAL ECD (PDB: 5VZ4) and zoom in on the binding interface of the C-terminal hairpin (green) of GDF15 with the D2 domain of GFRAL. The overlapping sequence (279–301) of the fragments that showed binding on SPOT array 2 is coloured blue. Sticks indicate amino acids important for binding to GFRAL as described by Hsu et al. (2017). Data are represented as mean \pm SD, $n = 2$.

Compounds were prepared in FBS-free cell medium with 0.1 % BSA. For testing peptide antagonists, GDF15 (Catalog# 957-GD-025, R&D systems) at fixed concentration (0.3 nM), corresponding to approximately EC_{90} , was added to the stimulation buffer. As controls, cells were stimulated \pm GDF15 in the absence of test compound. 16–24 h after transfection, the medium was discarded, and cells were stimulated for 15 min at 37 °C. ERK phosphorylation levels were measured using phospho-ERK (Thr202/Tyr204) cellular kit HTRF (Catalog# 64ERKPEH, Cisbio), where the assay reagents were added as per the manufacturer's instructions and time-resolved fluorescence energy transfer recorded after

2 h antibody incubation in a CLARIOstar Plus microplate reader (BMG Labtech, Ortenberg, Germany).

3. Results

3.1. GDF15 peptide fragments bind to the GFRAL extracellular domain

The crystal structure of GDF15 in complex with the GFRAL extracellular domain (ECD) revealed direct interactions of the N- and C-terminal hairpins of GDF15 with the D2 domain of GFRAL [22]. This

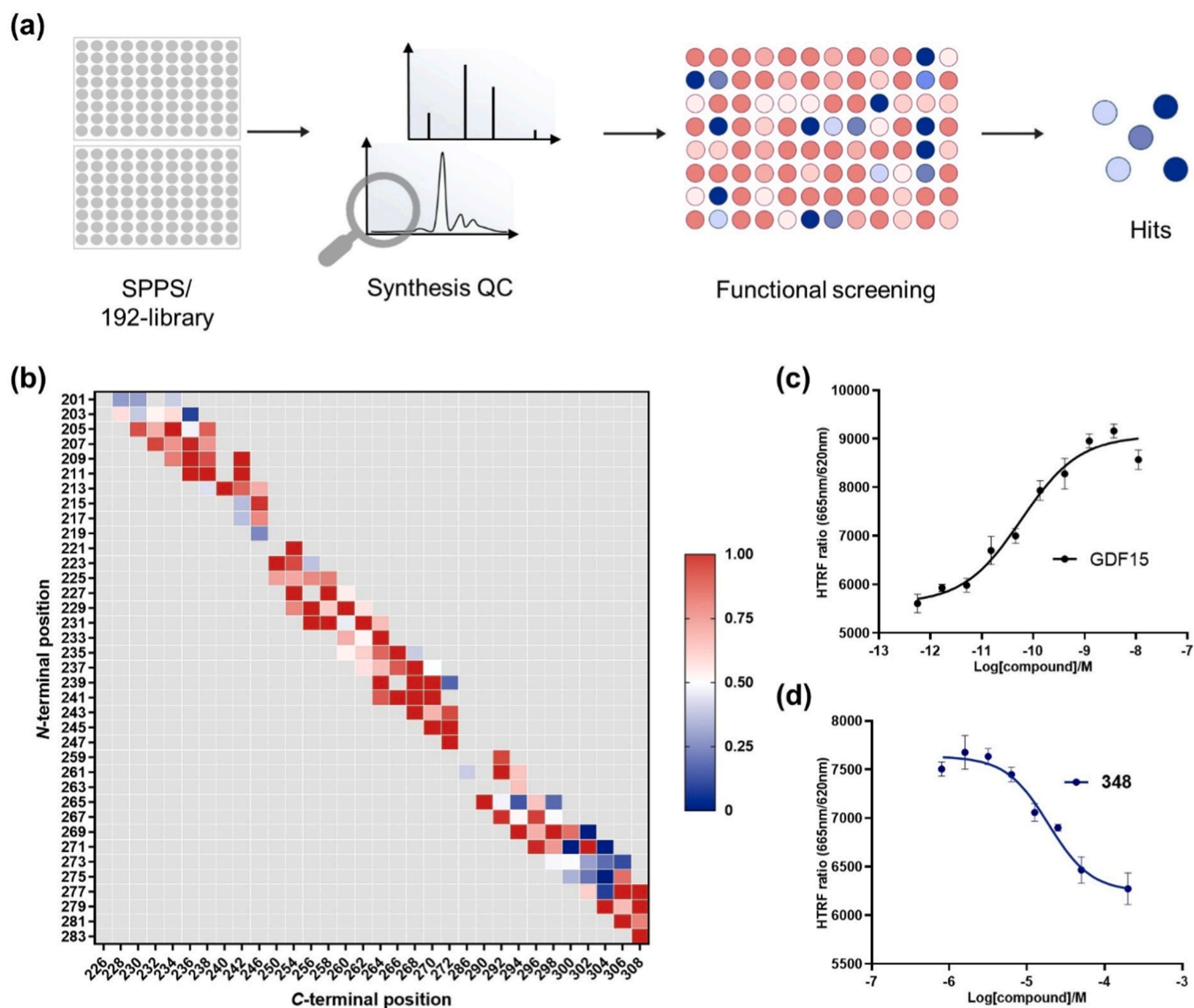


Fig. 2. C-hairpin GDF15 peptide fragments inhibit GFRAL signaling. (a) Schematic representation of functional screening workflow. A library of 192 peptides is synthesized using solid phase peptide synthesis (SPPS). After quality control analysis, peptides were screened in a single-point determination for their effect on GDF15 signaling. (b) Heatmap of normalized in vitro data of functional screening of GDF15 fragments (26–34-mers). Monoclonal GFRAL cells were transiently transfected with RET and stimulated with constant concentration of GDF15 ($EC_{85} = 0.3$ nM) and peptide ($C_{peptide} = 50$ μ M). Each square represents a peptide fragment plotted based on its N-terminal (x-axis) and C-terminal position (y-axis) based on the GDF15 sequence (201–308). GDF15 signaling (max signal = 1, red) is inhibited (min signal = 0, blue) by peptides deriving from the C-terminal region of GDF15. Peptides failed in synthesis are not included in the analysis, data are based on $n = 1$. Representative examples of concentration-response curves of (c) GDF15 and (d) 348 (273–304) on monoclonal GFRAL cells transiently transfected with RET. Data are represented as mean \pm SD, $n = 3$.

finding prompted us to explore whether peptide fragments of GDF15 could mimic binding to GFRAL ECD. For this purpose, we employed SPOT peptide arrays for the parallel synthesis of GDF15 peptide fragments on functionalized cellulose membranes. SPOT arrays displaying GDF15 fragments were subsequently screened for binding to the GFRAL ECD (Fig. 1A).

First, the GDF15 sequence (GDF15_{201–308}) was screened by synthesizing on SPOT 15-mer GDF15 peptides (SPOT array 1). The array was designed by fragmenting GDF15 starting from the N-terminus and moving towards the C-terminus with shifting of 1 amino acid at a time (Table S1). Screening of SPOT array 1 against the GFRAL ECD revealed that the two strongest peptide binders (**88** ²⁸⁷KTDGTGVS³⁰¹ and **89** ²⁸⁸TDTGVSLQTYDDLLA³⁰²) derived from the C-terminal region of GDF15 (Fig. 1B and Fig. S1A). From the X-ray crystal structure of GDF15 in complex with GFRAL ECD, it was observed that the binding

sequence of **88** and **89** (residues 288–302) was part of the binding interface formed by the C-terminal hairpin of GDF15 and the D2 domain of GFRAL.

Next, we focused on the C-terminal region of GDF15, and a second array (SPOT array 2) was designed to enable a more thorough screening of the C-hairpin sequence (residues 273–308). Longer peptide fragments (16–23-mers) were synthesized, and C-hairpin was screened by shifting of 1 amino acid between peptides while moving towards the C-terminus (Table S3). Subsequent array screening showed various peptide binders to the GFRAL ECD (Fig. 1C, Fig. S1B). Interestingly, all binders shared overlapping sequences covering the complementary β -strands of the GDF15 C-hairpin (residues 279–301, Fig. 1D).

Following, an in vitro cell based functional assay (ERK phosphorylation) was established for the evaluation of the functional properties of the identified GDF15 peptide binders on GFRAL signaling. The two top

Table 1

Sequences and potency data of GDF15 fragments. All peptides are C-terminally amidated. Data are presented as mean \pm SD, $n = 3$; X indicates substitution of methionine with norleucine; N.D. for $EC_{50} > 200 \mu\text{M}$.

Peptide technology	Peptide No	GDF15 residues	EC_{50} (μM)	Sequence
SPOT	195	(283–301)	> 100	²⁸³ VLIQKTDGTGVSLSQTYDDL ³⁰¹
SPOT	253	(279–301)	51.6 ± 10.5	²⁷⁹ YNPMVLIQKTDGTGVSLSQTYDDL ³⁰¹
SPPS	311	(271–304)	25.2 ± 5.7	²⁷¹ APCCVPASYNPNleLIQKTDGTGVSLSQTYDDLAKD ³⁰⁴
SPPS	333	(241–272)	N.D.	²⁴¹ IGACPSQFRAANXHAQIKTSLHRLKPDTPAP ²⁷²
SPPS	348	(273–304)	19.1 ± 6.6	²⁷³ CCVPASYNPNXVLIQKTDGTGVSLSQTYDDLAKD ³⁰⁴
SPPS	387	(275–304)	> 100	²⁷⁵ VPASYNPNXVLIQKTDGTGVSLSQTYDDLAKD ³⁰⁴
SPPS	469	(273–304)	25.1 ± 15.7	²⁷³ SSVPASYNPNXVLIQKTDGTGVSLSQTYDDLAKD ³⁰⁴

hits from SPOT array 2, (**195** ²⁸³VLIQKTDGTGVSLSQTYDDL³⁰¹ and **253** ²⁷⁹YNPMVLIQKTDGTGVSLSQTYDDL³⁰¹) were synthesized and their ability to inhibit GFRAL signaling was evaluated in monoclonal GFRAL HEK cells transiently expressing the co-receptor RET. In the presence of constant concentration of GDF15 ($EC_{85} = 0.3 \text{ nM}$, Fig. 2C), both peptides showed weak inhibition of GFRAL, with **253** showing slightly higher potency ($EC_{50} = 51.6 \pm 10.5 \mu\text{M}$) than **195** ($EC_{50} > 100 \mu\text{M}$) (Table 1).

3.2. C-terminal GDF15 fragments inhibit GFRAL

After identifying GFRAL peptide binders using SPOT arrays, we decided to screen a complementary library of GDF15 fragments for their effect on GFRAL signaling. This allowed the synthesis of peptide libraries using solid-phase peptide synthesis (SPPS) and provided the additional advantage of investigating longer GDF15 peptide fragments than the ones displayed on SPOT arrays. A library of 192 peptides was designed where the GDF15 sequence (GDF15_{201–308}) was screened with peptides of various lengths (34, 32, 30, 28 and 26 amino acids), with shifting of 2 amino acids between peptides while moving from the N- to C-terminus (Table S5). Additionally, oxidation-prone methionine residues were substituted with norleucine (Nle) to optimize synthetic efficiency.

Peptide synthesis was followed by quality control analysis where 7–8 representative peptides of each length were selected for resolving their purity and concentration using liquid chromatography-mass spectrometry (LC-MS) and charged aerosol detector (CAD), respectively. An average peptide purity and concentration was calculated, based on which peptides were aliquoted for functional screening (Table S6). Next, all 192 peptides were analysed by LC-MS and peptides for which their mass was not detected (71 out of 192) were excluded from analysis (Table S5).

Functional screening was performed on GFRAL/RET cells, in a single-point determination ($C_{\text{peptide}} = 50 \mu\text{M}$) in the presence of a fixed concentration of GDF15 ($EC_{85} = 0.3 \text{ nM}$) (Fig. 2A). This screening procedure indicated that a subset of peptides deriving from the C-terminal region of GDF15 (271–304) consistently inhibited GFRAL signaling (Fig. 2B). A series of fragments across the GDF15 sequence were then selected for individual LC-MS and CAD analysis and subsequently characterized in a 5-point crude peptide concentration-response assay. In agreement with the initial library screening, it was observed that 30–34 amino acid C-hairpin peptide fragments **311**, **348** and **386** sharing the sequence 271–304 could inhibit GFRAL with a potency (EC_{50}) of up to $32 \mu\text{M}$ (Table S7).

3.3. In vitro validation of GFRAL inhibitors

Since screening was performed with crude peptides, validation of the findings was required. Three hit peptides of different lengths (²⁷¹APCCVPASYNPNleLIQKTDGTGVSLSQTYDDLAKD³⁰⁴ **311**, ²⁶⁹CCVPA SYNPNleVLIQKTDGTGVSLSQTYDDLAKD³⁰⁴ **348**, ²⁶⁷VPASYNPNleVLIQKTDGTGVSLSQTYDDLAKD³⁰⁴ **387**) and a peptide fragment showing no inhibition (²⁴¹IGACPSQFRAANleHAQIKTSLHRLKPDTPAP²⁷² **333**) were selected for synthesis, purification, and in vitro validation of their functional properties (Table 1, Table S8).

Similar to the potency data obtained with crude peptides (Table S7), concentration-response curves of **311** and **348** showed that these were the most potent GFRAL inhibitors ($EC_{50} = 25.2 \pm 3.7$ and $19.1 \pm 6.6 \mu\text{M}$ respectively, Fig. 2D), while **333** did not show receptor inhibition (Table 1). Additionally, the shortest analogue **387** with an N-terminal deletion of two cysteine residues, Cys273 and Cys274, resulted in loss of receptor potency ($EC_{50} > 100 \mu\text{M}$, Table 1). Finally, we evaluated whether increased potency of **311** and **348** could be attributed to peptide dimerization via disulphide bridge formation under the assay conditions. A serine substituted analogue of **348** (²⁶⁹SSVPAS YNPNleVLIQKTDGTGVSLSQTYDDLAKD³⁰⁴) **469** showed similar antagonistic profile ($EC_{50} = 25.1 \pm 15.7$, Table 1) to **348** indicating that the GDF15 peptide fragment **348** is the most potent inhibitor of the GFRAL. Last, **348**, its shorter analogue **195** and the inactive peptide **333** were evaluated for receptor agonism showing no GFRAL activation (Fig. S2).

4. Discussion

GDF15 is well documented for playing a critical role in driving uncontrollable and severe loss of body weight in patients with cancer [32, 33]. Here, we report the application of peptide screening platforms for the discovery of novel GDF15 peptide fragments that inhibit GFRAL signaling, thus providing valuable tools for the in vivo elucidation of GFRAL inhibitory effects as well as the development of peptide therapeutics towards the treatment of cancer cachexia.

The binding properties of GDF15 peptide fragments to the GFRAL ECD were investigated utilizing SPOT peptide arrays. The initial screening of the GDF15 sequence revealed binding of two 15-mer peptides (**88** and **89**, residues 287–302) derived from the C-terminal hairpin (residues 274–308) of GDF15. Interestingly, GFRAL binders included residues (e.g. Thr290, Val292) reported to mediate intermolecular contacts ($\leq 4.5 \text{ \AA}$) between GDF15 C-hairpin and the D2 domain of GFRAL [22]. Subsequent screening of 16–23-mer fragments demonstrated consistent C-terminal binders sharing an extended overlapping sequence (residues 277–302). Collectively, these data suggested that C-terminal fragments covering residues of the complementary β -strands of the GDF15 C-hairpin could bind with increasing affinity to the GFRAL ECD. Functional evaluation of two selected binders (**195** and **253**) in cells co-expressing GFRAL/RET showed weak inhibition of GDF15-induced signaling.

SPOT peptide arrays offer a powerful method for the identification of binding epitopes and targeting of protein-protein interactions [34], though the synthetic efficiency is highly dependent on the peptide sequence, length and potential secondary structure. Low synthetic yields observed for C-terminal GDF15 fragments longer than 20 amino acids limited the application of SPOT arrays for the investigation of the binding properties of long GDF15 peptide fragments. For this purpose, we applied a parallel SPPS method that allowed a complementary screening of GDF15 peptide fragments ranging from 26 to 34 amino acids. Due to high diversity of peptide sequences and lengths, variation on synthesis yield of individual peptides was observed. Hence, thorough quality control analysis was performed allowing unbiased processing and interpretation of the peptide screening data. In agreement with SPOT data, functional screening of long GDF15 peptide fragments in

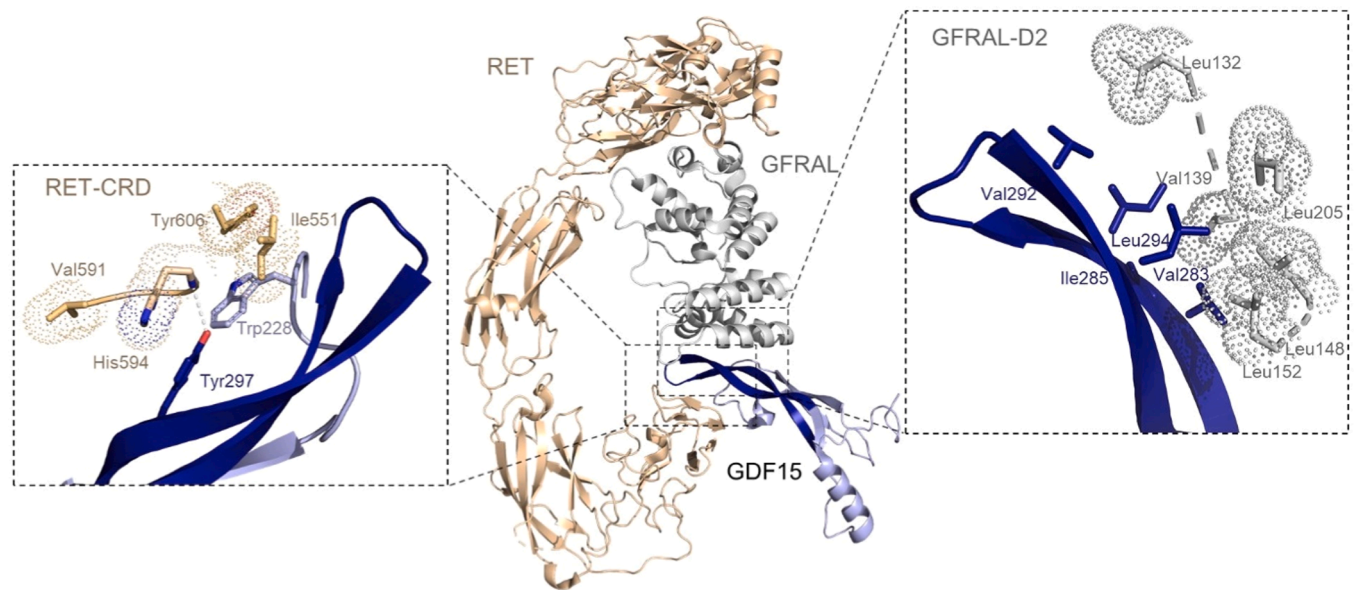


Fig. 3. Cryo-EM structure of GDF15 monomer in complex with GFRAL ECD and co-receptor RET. The GFRAL peptide inhibitor **348** (blue) is derived from the C-terminal hairpin of GDF15 that forms an extensive hydrophobic interface with the D2 domain of GFRAL extracellular domain (grey). Opposite to the GFRAL/GDF15 interaction site, GDF15 interacts with the cysteine rich domain (CRD) of the co-receptor RET (orange) through hydrophobic interactions. Important for binding to GFRAL and RET amino acids are shown in sticks (PDB: 6q2j).

GFRAL/RET cells indicated inhibition of GFRAL signaling with peptides deriving from the C-hairpin of GDF15. We observed that fragments **311**, **348** and **387** sharing Asp304 as the C-terminal residue, consistently inhibited GFRAL. Consequently, these peptides were synthesized, purified and functionally evaluated, resulting on the identification of **348** (residues 273–304) as the most potent GFRAL inhibitor ($EC_{50} = 19.1 \pm 6.6 \mu\text{M}$).

We hypothesize that **348** inhibits GFRAL by disrupting the GDF15/GFRAL interface. This hypothesis is supported by previously reported structural information of GDF15 in complex with GFRAL ECD, indicating that the amino acid residues of **348** (273–304) form an extensive binding interface between the C-hairpin of GDF15 and a hydrophobic pocket on the D2 domain of GFRAL ECD (Fig. 3) [22,35]. Importantly, Hsu et al. demonstrated that hydrophobic interactions formed by Val283 and Ile285 are critical for GDF15/GFRAL interaction as single point mutations in these residues (V83A and I85A) reduced GDF15-dependent signaling. Additionally, Li et al. reported a cryo-EM structure of the extracellular ternary complex of GDF15/GFRAL/RET revealing a binding interface between GDF15 and the C-terminal cysteine rich domain (CRD) of RET [35]. The RET/GDF15 interaction site appears opposite to the GFRAL/GDF15 site resulting in a ‘sandwich’ formation between RET, GDF15 and GFRAL. The RET-CRD interacts mainly through hydrophobic contacts with the N- and C-hairpin loops of GDF15 (Fig. 3). Interestingly, mutation of Tyr297 (Y297E) in GDF15 abolished the formation of the ternary complex and dramatically decreased phosphorylation of ERK. We therefore hypothesize that **348** could inhibit GFRAL signaling through disruption of both the GDF15/GFRAL and GDF15/RET interface.

In summary, this study reports the application of two complementary peptide technologies, SPOT peptide arrays and functional screening, for the focused identification of GDF15 peptide fragments inhibiting the GFRAL/RET receptor complex. We here describe, for the first time, peptide inhibitors of GFRAL, though the pharmacological potential of these peptides remains to be investigated, including binding affinity to the extracellular domains of GFRAL and RET. Also, identification of amino acid residues essential for receptor binding will potentially contribute to the optimization of the inhibitory potency of GDF15 peptides. It should be noted that the native structural conformation of the GFRAL/RET receptor complex could be essential for determination

of peptide binding and receptor inhibition. Additionally, introduction of conformational constraints locking the peptide into a hairpin conformation may potentially improve the pharmacological properties of GFRAL peptide inhibitors. We hope that this study will encourage further investigations towards the development of GFRAL peptide antagonists, opening new directions for in vivo elucidation of GFRAL inhibition in various diseases, notably cancer cachexia and other anorectic conditions. While it is well-established that cancer cells overexpress and secrete GDF15, it should be noted that GDF15 may play a complex role in tumorigenesis as GDF15 has been reported to suppress growth of certain early tumor types while stimulating tumor growth in advanced cancer [36]. Future studies must aim to profile GFRAL peptide antagonists for effects on appetite function.

Author contributions

F.A., N.B.M., S.L.P., L.N.F., N.V. and K.S. conceived and designed experiments. F.A. performed experiments, F.A. and N.B.M. analysed and interpreted data. F.A. wrote the manuscript. All authors reviewed and approved the final manuscript.

Declaration of Competing Interest

F.A., N.B.M., and L.N.F. are employed by Gubra; S.L.P. was previously employed by Gubra; N.V. is co-founder of Gubra.

Data availability

Data will be made available on request.

Acknowledgments

This work was supported by a PhD grant (Flora Alexopoulou) from Innovation Fund Denmark (grant no. 9065-00138B) and Danish Diabetes Academy which is funded by the Novo Nordisk Foundation (grant no. NNF17SA0031406).

Appendix A. Supporting information

Supplementary data associated with this article can be found in the online version at [doi:10.1016/j.peptides.2023.171063](https://doi.org/10.1016/j.peptides.2023.171063).

References

- [1] M.R. Bootcov, et al., MIC-1, a novel macrophage inhibitory cytokine, is a divergent member of the TGF- β superfamily, *Proc. Natl. Acad. Sci. U. S. A.* 94 (1997) 11514–11519.
- [2] L.N. Lawton, et al., Identification of a novel member of the TGF-beta superfamily highly expressed in human placenta, *Gene* 203 (1997) 17–26.
- [3] R. Hromas, et al., PLAB, a novel placental bone morphogenetic protein, *Biochim. Biophys. Acta - Gene Struct. Expr.* 1354 (1997) 40–44.
- [4] W.D. Fairlie, et al., MIC-1 is a novel TGF- β superfamily cytokine associated with macrophage activation, *J. Leukoc. Biol.* 65 (1999) 2–5.
- [5] F.E. Wiklund, et al., Macrophage inhibitory cytokine-1 (MIC-1/GDF15): a new marker of all-cause mortality, *Aging Cell* 9 (2010) 1057–1064.
- [6] A.G. Moore, et al., The transforming growth factor- β superfamily cytokine macrophage inhibitory cytokine-1 is present in high concentrations in the serum of pregnant women, *J. Clin. Endocrinol. Metab.* 85 (2000) 4781–4788.
- [7] M. Kleinert, et al., Exercise increases circulating GDF15 in humans, *Mol. Metab.* 9 (2018) 187–191.
- [8] H.H. Luan, et al., GDF15 is an inflammation-induced central mediator of tissue tolerance, 1231-1244.e11, *Cell* 178 (2019), 1231-1244.e11.
- [9] J.B. Welsh, et al., Large-scale delineation of secreted protein biomarkers overexpressed in cancer tissue and serum, *Proc. Natl. Acad. Sci. U. S. A.* 100 (2003) 3410–3415.
- [10] T. Kempf, et al., Prognostic utility of growth differentiation factor-15 in patients with chronic heart failure, *J. Am. Coll. Cardiol.* 50 (2007) 1054–1060.
- [11] S.N. Breit, et al., Macrophage inhibitory cytokine-1 (MIC-1/GDF15) and mortality in end-stage renal disease, *Nephrol. Dial. Transplant.* 27 (2012) 70–75.
- [12] E.S. Lee, et al., Growth differentiation factor 15 predicts chronic liver disease severity, *Gut Liver* 11 (2017) 276–282.
- [13] D.S. Ahmed, et al., Coping with stress: The mitokine GDF-15 as a biomarker of COVID-19 severity, *Front. Immunol.* 13 (2022), 820350.
- [14] I. Dostálová, et al., Increased serum concentrations of macrophage inhibitory cytokine-1 in patients with obesity and type 2 diabetes mellitus: the influence of very low calorie diet, *Eur. J. Endocrinol.* 161 (2009) 397–404.
- [15] H. Johnen, et al., Tumor-induced anorexia and weight loss are mediated by the TGF- β superfamily cytokine MIC-1, *Nat. Med.* 13 (2007) 1333–1340.
- [16] W.D. DeWys, Pathophysiology of cancer cachexia: Current understanding and areas for future research, *Cancer Res.* 42 (1982) 721–726.
- [17] K. Fearon, et al., Definition and classification of cancer cachexia: an international consensus, *Lancet Oncol.* 12 (2011) 489–495.
- [18] J.M. Argilés, S. Busquets, B. Stemmler, F.J. López-Soriano, Cancer cachexia: Understanding the molecular basis, *Nat. Rev. Cancer* 14 (2014) 754–762.
- [19] K.C.H. Fearon, D.J. Glass, D.C. Guttridge, Cancer cachexia: mediators, signaling, and metabolic pathways, *Cell Metab.* 16 (2012) 153–166.
- [20] V.E. Baracos, L. Martin, M. Korc, D.C. Guttridge, K.C.H. Fearon, Cancer-associated cachexia, *Nat. Rev. Dis. Prim.* 4 (2018) 1–18.
- [21] W.J. Evans, et al., Cachexia: a new definition, *Clin. Nutr.* 27 (2008) 793–799.
- [22] J.Y. Hsu, et al., Non-homeostatic body weight regulation through a brainstem-restricted receptor for GDF15, *Nature* 550 (2017) 255–259.
- [23] S.E. Mullican, et al., GFRAL is the receptor for GDF15 and the ligand promotes weight loss in mice and nonhuman primates, *Nat. Med.* 23 (2017) 1150–1157.
- [24] L. Yang, et al., GFRAL is the receptor for GDF15 and is required for the anti-obesity effects of the ligand, *Nat. Med.* 23 (2017) 1158–1166.
- [25] P.J. Emmerson, et al., The metabolic effects of GDF15 are mediated by the orphan receptor GFRAL, *Nat. Med.* 23 (2017) 1215–1219.
- [26] C.F.W. Chow, et al., Body weight regulation via MT1-MMP-mediated cleavage of GFRAL, *Nat. Metab.* 4 (2022) 203–212.
- [27] Y. Xiong, et al., Long-acting MIC-1/GDF15 molecules to treat obesity: Evidence from mice to monkeys, *Sci. Transl. Med.* 9 (2017) 1–12.
- [28] O. Benichou, et al., Discovery, development, and clinical proof of mechanism of LY3463251, a long-acting GDF15 receptor agonist, e10, *Cell Metab.* 35 (2023) 274–286. e10.
- [29] R. Suriben, et al., Antibody-mediated inhibition of GDF15–GFRAL activity reverses cancer cachexia in mice, *Nat. Med.* 26 (2020) 1264–1270.
- [30] D.M. Breen, et al., GDF-15 neutralization alleviates platinum-based chemotherapy-induced emesis, anorexia, and weight loss in mice and nonhuman primates, e6, *Cell Metab.* 32 (2020) 938–950. e6.
- [31] B.Y. Lee, et al., GDNF family receptor alpha-like antagonist antibody alleviates chemotherapy-induced cachexia in melanoma-bearing mice, *J. Cachexia Sarcopenia Muscle* (2023).
- [32] L. Lerner, et al., Plasma growth differentiation factor 15 is associated with weight loss and mortality in cancer patients, *J. Cachexia Sarcopenia Muscle* 6 (2015) 317–324.
- [33] L. Lerner, et al., MAP3K11/GDF15 axis is a critical driver of cancer cachexia, *J. Cachexia Sarcopenia Muscle* 7 (2016) 467–482.
- [34] C. Katz, et al., Studying protein–protein interactions using peptide arrays, *Chem. Soc. Rev.* 40 (2011) 2131–2145.
- [35] J. Li, et al., Cryo-EM analyses reveal the common mechanism and diversification in the activation of RET by different ligands, *Elife* 8 (2019) 1–26.
- [36] D.S. Ahmed, S. Isnard, J. Lin, B. Routy, J.-P. Routy, GDF15/GFRAL pathway as a metabolic signature for cachexia in patients with cancer, *J. Cancer* 12 (2021) 1125–1132.